Local polarization distribution in quadrupolar glasses

B. Tadić, R. Pirc, and R. Blinc
Jožef Stefan Institute, P.O. Box 3000, 1001 Ljubljana, Slovenia
(Received 11 July 1996; revised manuscript received 23 September 1996)

We consider the semimicroscopic symmetry-adapted random-bond–random-field model of quadrupolar glasses such as NaCN:KCN and KBr:KCN, assuming strong lattice anisotropy which restricts the equilibrium orientations of the CN molecules to a set of discrete directions along the cubic ⟨100⟩ axes. Applying the replica theory of orientational glasses, we calculate the probability distribution $W(p_1,p_2)$ for the two independent components of local quadrupolar polarization p_1 and p_2 in the replica-symmetric quadrupolar glass phase. The reduced distributions $W_2(p_2)\equiv\int W(p_1,p_2)dp_1$ and $W_1(p_1)\equiv\int W(p_2,p_1)dp_2$ are shown to be related to the quadrupole-perturbed NMR line shape $I(\nu)$ of the ^{14}N nucleus. [S0163-1829(97)01802-X]

I. INTRODUCTION

Quadrupolar glasses (QG's) are random molecular crystals with specific physical properties, which are in many ways analogous to magnetic spin glasses.[1,2] The low-temperature phase of a QG is characterized by a random freezeout of molecular orientations and of the accompanying quadrupolar degrees of freedom.[3] Historically, among the first such systems to be studied were solid mixtures of ortho-para hydrogen.[4,5] More recently, there has been much theoretical[6–8] and experimental[9] interest in mixed alkali halide-cyanide systems, for example, $KBr_{1-x}(CN)_x$, $NaCl_{1-x}(CN)_x$, and related compounds, and in mixed alkali cyanides such as $(NaCN)_{1-x}(KCN)_x$. In the high-temperature phase, the average structure of these systems is cubic. In general, they are characterized by strong crystal anisotropy,[10] which restricts the rotational motion of CN molecules at temperatures below ~40 K to a set of equilibrium orientations, which are typically along the ⟨100⟩, ⟨111⟩, or ⟨110⟩ crystallographic direction. On a coarse-grained mesoscopic scale, compositional disorder in these systems gives rise to random interactions between the quadrupole moments, which are mediated by short-wavelength lattice vibrations.[6] Another feature, not having an analogy in spin glasses, is the occurrence of local random elastic fields acting on the orientational degrees of freedom.[11,12]

It has been shown earlier that the equilibrium properties of random systems containing bistable electric dipoles, such as proton and deuteron glasses, can be well described by the Ising random-bond–random-field (RBRF) model.[13] In a more general case of a QG with more than two discrete equilibrium orientations, the orientational fluctuations can be represented by a set of Potts variables,[14,6] which are simply related to the discrete-state occupation numbers. Specifically, for cubic systems with a ⟨100⟩, ⟨111⟩, or ⟨110⟩ equilibrium direction of the quadrupolar axis the appropriate choice is the RBRF s-state Potts model, where $s=3$, 4, or 6, respectively.[6] In analogy with dipolar glasses, the presence of random fields gives rise to a nonzero component of the QG order parameter in the high-temperature phase. However, the freezing phase transition into a nonergodic QG phase still exists, and can be interpreted as the onset of instability of the replica-symmetric QG phase below the freezing temperature T_f, which depends on the strength of the random strain fields.

Recently, the RBRF model of QG's has been formulated in terms of symmetry-adapted order parameter fields $Z_{i\mu}$ with $r=s-1$ relevant components, which are linear combinations of the Potts variables and transform according to the irreducible representations of the cubic group.[8,15] This formulation has been motivated by the following facts: (i) Local random strains can be uniquely represented by their irreducible components, which are linearly coupled to the order parameter fields of the same symmetry; (ii) in experimental studies of the elastic behavior, irreducible stresses are applied[9] and the response due to the quadrupolar degrees of freedom of the same symmetry is monitored; (iii) the NMR line shape is for certain directions of the magnetic field directly related to the probability distribution for the symmetrized components of the local quadrupolar polarization. As shown earlier for dipolar glasses,[16] quadrupole-perturbed NMR and related techniques are suitable for monitoring the temperature dependence of the quadrupolar Edwards-Anderson order parameter $q_{\rm EA}(T)$. In the mixed cyanide systems $Na(CN)_xCl_{1-x}$ and $(NaCN)_{1-x}(KCN)_x$, $q_{\rm EA}(T)$ has been determined from the second moments of the NMR spectra of ^{35}Cl and ^{23}Na.[17] A more recent investigation is based on the quadrupole-perturbed NMR spectrum of the ^{14}N nucleus,[18] which directly follows the orientation of the CN quadrupolar axis.

To our knowledge, a complete theory of the NMR line shape of a QG based on the appropriate microscopic model has not yet been worked out. Here we consider the mixed cyanide systems and apply the symmetry-adapted random-bond–random-field (SARBRF) model in order to calculate the NMR line shape within a replica mean-field theory. Since in the range of concentrations where QG behavior is observed the most probable equilibrium orientation of the CN quadrupolar axis is along the three cubic ⟨100⟩ directions,[10] we will focus on the $r=2$ SARBRF model with two relevant quadrupolar degrees of freedom. These are associated with the two independent components of the local quadrupolar polarization, namely, p_1 and p_2. The problem then reduces to calculating the probability distribution $W(p_1,p_2)$ for these two components, which can be simply related to the NMR spectrum. For a specific direction of the external magnetic

field, the NMR spectrum depends on one of these variables only, and is thus determined by the reduced probability distribution obtained by integrating out the remaining component. We will consider explicitly those orientations, which are relevant to the quadrupole-perturbed NMR of the ^{14}N nucleus of the CN molecule in $(NaCN)_{1-x}(KCN)_x$.[18]

The organization of the paper is as follows: In Sec. II we outline the mean-field theory of the static properties of QG's.[15] In Sec. III we calculate the probability distribution $W(p_1,p_2)$ in the entire space of local quadrupolar polarization components p_1 and p_2, from which the reduced distributions $W_\mu(p_\mu)$ ($\mu=1,2$) are then obtained. In Sec. IV, the relation between the NMR line shape $I(\nu)$ and $W_\mu(p_\mu)$ in the slow- and fast-motion limits is derived. Section V contains a short summary and discussion.

II. EQUILIBRIUM PROPERTIES OF A QUADRUPOLAR GLASS

A. SARBRF model

In the case of strong crystal anisotropy, such as in $(NaCN)_{1-x}(KCN)_x$ and related compounds, the equilibrium orientations of the quadrupolar axis of the CN molecules are along the $\langle 100\rangle$, $\langle 111\rangle$, or $\langle 110\rangle$ crystallographic direction of a cubic lattice. As usual,[6] we will ignore the head-to-tail electric dipolar degrees of freedom; thus the corresponding number of equilibrium orientations for the above three cases will be equal to $s=3$, 4, or 6, respectively. The occupation number N_{im} for the mth orientation of the ith quadrupole can thus have the value 0 (unoccupied) or 1 (occupied), with $m=1,2,\ldots,s$. In order to describe the equilibrium properties of QG's of the above type we adopt the SARBRF model of orientational glasses,[8,15]

$$\mathcal{H}=-\frac{1}{2}\sum_{ij} J_{ij}\sum_{\mu=1}^{r} Z_{i\mu}Z_{j\mu}-\sum_i \sum_{\mu=1}^{r}(h_{i\mu}+E_\mu)Z_{i\mu}, \tag{1}$$

which is formulated in terms of the symmetry-adapted order-parameter fields $Z_{i\mu}$, where $\mu=1,2,\ldots,r$, with $r=1-s$, labels the irreducible representations of the cubic group (for a discussion of discrete-state models appropriate to orientational glasses of various symmetries see Ref. 15, to be referred to as I). The fields $Z_{i\mu}$ will be defined here as linear combinations of the Potts variables $\hat{N}_{im}\equiv N_{im}-1/s$ rather than occupation numbers N_{im}.[15] Thus we write

$$Z_{i\mu}=\sum_{m=1}^{s} a_{\mu m}\hat{N}_{im}. \tag{2}$$

The Potts variables $\hat{N}_{im}$ satisfy the closure relation

$$\sum_{m=1}^{s}\hat{N}_{im}=0. \tag{3}$$

Therefore, one has $Z_{is}\equiv\Sigma_{m=1}^{s}\hat{N}_{im}=0$, and there are only $r=s-1$ nontrivial fields $Z_{i\mu}$ ($\mu=1,2,\ldots,r$).

The coefficients $a_{\mu m}$ in Eq. (2), which are elements of an $r\times s$ matrix, are fixed by group theory and can be identified from the following explicit relations (we drop the site indices i) for the three cubic cases:

$$\langle 100\rangle:\quad Z_1=\sqrt{\tfrac{3}{2}}(\hat{N}_1-\hat{N}_2),\quad Z_2=\sqrt{\tfrac{1}{2}}(2\hat{N}_3-\hat{N}_1-\hat{N}_2); \tag{4}$$

$$\langle 111\rangle:\quad Z_1=\hat{N}_1+\hat{N}_2-\hat{N}_3-\hat{N}_4,\quad Z_2=\hat{N}_2+\hat{N}_3-\hat{N}_1-\hat{N}_4,$$
$$Z_3=\hat{N}_3+\hat{N}_1-\hat{N}_2-\hat{N}_4; \tag{5}$$

$$\langle 110\rangle:\quad Z_1=\sqrt{\tfrac{3}{2}}(\hat{N}_2+\hat{N}_5-\hat{N}_3-\hat{N}_6),$$
$$Z_2=\sqrt{\tfrac{1}{2}}(2\hat{N}_1+2\hat{N}_4-\hat{N}_2-\hat{N}_3-\hat{N}_5-\hat{N}_6),$$
$$Z_3=\sqrt{3}(\hat{N}_1-\hat{N}_4),\quad Z_4=\sqrt{3}(\hat{N}_2-\hat{N}_5),$$
$$Z_5=\sqrt{3}(\hat{N}_3-\hat{N}_6). \tag{6}$$

The normalization in Eqs. (4)–(6) is chosen in such a way that

$$\sum_{\mu=1}^{r} Z_{i\mu}^2=r. \tag{7}$$

One can readily write down the inverse relations

$$\hat{N}_{im}=\frac{1}{s}\sum_{\mu=1}^{r} a_{m\mu}^T Z_{i\mu}, \tag{8}$$

where $a_{m\mu}^T=a_{\mu m}$, which should be supplemented by the closure relation (3).

In Eq. (1), the compositional disorder leading to QG behavior is represented by quenched random infinite-range interactions J_{ij} and and local random fields $h_{i\mu}$, which are assumed to be uncorrelated and described by a joint Gaussian distribution with mean values $[(J_{ij})]_{\rm av}=J_0/N$ and $[h_{i\mu}]_{\rm av}=0$ and with variances $[(J_{ij})^2]_{\rm av}=J^2/N$ and $[h_{i\mu}h_{j\nu}]_{\rm av}=\Delta J^2\delta_{ij}\delta_{\mu\nu}$, respectively.

Formally, model (1) is also applicable to Ising dipolar glasses, where one has $s=2$ or $r=1$ and $Z_{i1}=\hat{N}_{i1}-\hat{N}_{i2}\equiv S_i=\pm 1$.

As discussed in more detail in Sec. IV, the quantities of interest in NMR and related experiments are the quadrupolar polarizations

$$P_\mu=\frac{1}{N}\sum_i \langle Z_{i\mu}\rangle=[\langle Z_{i\mu}\rangle]_{\rm av}, \tag{9}$$

where N is the number of CN molecules, $\langle\cdots\rangle$ represents the thermal average, and $[\cdots]_{\rm av}$ the random average. Equation (9) is a straightforward generalization of the local polarization in Ising dipolar glasses.[16] In further analogy with dipolar glasses one can introduce the quadrupolar Edwards-Anderson (EA) order parameters

$$q_\mu^{\rm EA}=\frac{1}{N}\sum_i \langle Z_{i\mu}\rangle^2=[\langle Z_{i\mu}\rangle^2]_{\rm av}. \tag{10}$$

B. $\langle 100\rangle$ case: Results of replica theory

In the following we will focus on the $\langle 100\rangle$ orientation model ($r=2$) and briefly review some of the results of replica theory,[14] which are relevant to further discussion. As discussed in more detail in I, in the replica-symmetric QG phase the problem reduces to an effective single-site system

in a vector Gaussian random field $\vec{x}=(x_1,x_2,x_3)$. Alternatively, one can derive equivalent results without the use of replicas from a dynamic theory, where $\vec{x}$ is interpreted as a static excess noise field.[19] The average free energy per CN molecule is thus given by

$$f=-\tfrac{1}{4}\beta^2J^2[(q_1-1)^2+(q_2-1)^2+2q_T]+\tfrac{1}{2}\beta J_0^{\rm eff}(P_1^2+P_2^2)$$
$$-(2\pi)^{-3/2}\int_{-\infty}^{+\infty}dx_1\int_{-\infty}^{+\infty}dx_2\int_{-\infty}^{+\infty}dx_3$$
$$\times\exp(-\vec{x}^2/2)\ln g(H_1,H_2), \tag{11}$$

where $J_0^{\rm eff}\equiv J_0+\beta J^2/2$ and we have introduced the local partition function

$$g(H_1,H_2)=2\cosh(\sqrt{3/2}\beta H_1)\exp(-\beta H_2/\sqrt{2})$$
$$+\exp(\sqrt{2}\beta H_2), \tag{12}$$

with effective local fields $H_\mu=H_\mu(\vec{x})$ $(\mu=1,2)$:

$$H_1=J(q_1+\Delta-q_T)^{1/2}x_1+Jq_T^{1/2}x_3+J_0^{\rm eff}P_1+(\sqrt{2}/2)\beta J^2q_T,$$
$$H_2=J(q_2+\Delta-q_T)^{1/2}x_2+Jq_T^{1/2}x_3+J_0^{\rm eff}P_2$$
$$+(\sqrt{2}/4)\beta^2J^2(q_1-q_2). \tag{13}$$

In terms of these variables the local quadrupolar polarizations can be expressed as

$$\hat{p}_\mu(\vec{x})=\partial\ln g/\partial(\beta H_\mu)\quad(\mu=1,2). \tag{14}$$

The conditions $\partial f/\partial P_1=\cdots=\partial f/\partial q_T=0$ then lead to a set of coupled equations for the order parameters, P_μ, q_μ, and q_T. These can be written in compact form in terms of the above local polarizations $\hat{p}_1(\vec{x})$ and $\hat{p}_2(\vec{x})$, namely,

$$P_\mu=[\hat{p}_\mu(\vec{x})]_{\vec{x}},\quad q_\mu=[\hat{p}_\mu^2(\vec{x})]_{\vec{x}},\quad q_T=[\hat{p}_1(\vec{x})\hat{p}_2(\vec{x})]_{\vec{x}}. \tag{15}$$

The symbol $[\cdots]_{\vec{x}}$ means a triple Gaussian average over the variables x_1, x_2, and x_3. The replica-symmetric order parameter q_μ is a measure of the physically relevant quadrupolar Edwards-Anderson order parameter $q_\mu^{\rm EA}$.

We are interested in the QG phase without long-range ferroelastic order, i.e., $P_\mu=0$. It turns out that in practical applications one can always find a range of temperatures and concentrations x for which $J_0^{\rm eff}=0$ and thus no long-range order appears, as indeed seems to be the case in mixed cyanide systems.[10] The problem of long-range order can be avoided[19] by replacing the isotropic scalar interaction J_{ij} in Eq. (1) by a general randomly anisotropic interaction $J_{ij}^{\mu\nu}$; however, we will not enter a discussion of this alternative here.

The temperature and random-field dependences of the order parameters q_μ and q_T can be calculated from the above expressions and are given in detail in I (see Figs. 1 and 2 of I). It is also shown there that in the replica-symmetric QG phase one has $q_T=0$, which eliminates the Gaussian integration over x_3. Moreover, the diagonal components of the replica-symmetric quadrupolar order parameter q_μ are equal, i.e., $q_\mu=q$ for $\mu=1$ and 2, so that one is left with a single QG order parameter q.

III. DISTRIBUTION OF LOCAL QUADRUPOLAR POLARIZATIONS

The probability distribution of local quadrupolar polarizations for the $\langle 100\rangle$ case is generally defined as

$$\tilde{W}(\hat{p}_1,\hat{p}_2)=\frac{1}{N}\sum_i\ \delta(\hat{p}_1-\langle Z_{i1}\rangle)\,\delta(\hat{p}_2-\langle Z_{i2}\rangle). \tag{16}$$

In the replica theory, it turns out to be more convenient to deal with rescaled local polarizations

$$p_1(\vec{x})=c_1\hat{p}_1(\vec{x}),\quad p_2(\vec{x})=c_2\hat{p}_2(\vec{x}), \tag{17}$$

where the purpose of the coefficients c_μ $(\mu=1,2)$ is to compensate the prefactors in Eq. (4), implying $c_1=\sqrt{2/3}$ and $c_2=\sqrt{2}$. The corresponding probability distribution can then be written as

$$W(p_1,p_2)=[\,\delta(p_1-p_1(\vec{x}))\,\delta(p_2-p_2(\vec{x}))]_{\vec{x}}. \tag{18}$$

In the replica-symmetric phase, according to Eqs. (12)–(14), the two independent local quadrupolar polarizations $p_1(\vec{x})$ and $p_2(\vec{x})$ are given by the following expressions:

$$p_1(\vec{x})=\frac{2\sinh(\sqrt{3/2}\beta H_1)}{R(H_1,H_2)}, \tag{19}$$

$$p_2(\vec{x})=2\frac{\exp(3\beta H_2/\sqrt{2})-\cosh(\sqrt{3/2}\beta H_1)}{R(H_1,H_2)}, \tag{20}$$

where

$$R(H_1,H_2)=2\cosh(\sqrt{3/2}\beta H_1)+\exp(3\beta H_2/\sqrt{2}), \tag{21}$$

with

$$H_\mu=J(q+\Delta)^{1/2}x_\mu\quad(\mu=1,2). \tag{22}$$

The random fields x_1 and x_2 are due to the combined effect of QG ordering, $q\neq0$, and local random strain fields, $\Delta\neq0$. On the level of a mean-field theory of QG's these fields are Gaussian [cf. Eq. (11)]. The double-Gaussian distribution of x_1 and x_2 determines the distribution of local polarization components $p_1(\vec{x})$ and $p_2(\vec{x})$ in the isotropic QG phase via Eqs. (19) and (20), which can be inverted to give $x_1(p_1,p_2)$ and $x_2(p_1,p_2)$. We find

$$x_1=a[\ln(2+3p_1-p_2)-\ln(2-3p_1-p_2)], \tag{23}$$

$$x_2=(2a/\sqrt{3})\{\ln(2+2p_2)$$
$$-\tfrac{1}{2}\ln[(2+3p_1-p_2)(2-3p_1-p_2)]\}, \tag{24}$$

where $a\equiv[\sqrt{6(q+\Delta)}\beta J]^{-1}$. Thus

$$W(p_1,p_2)=\frac{1}{2\pi}\mathcal{J}\exp(-x_1^2/2-x_2^2/2), \tag{25}$$

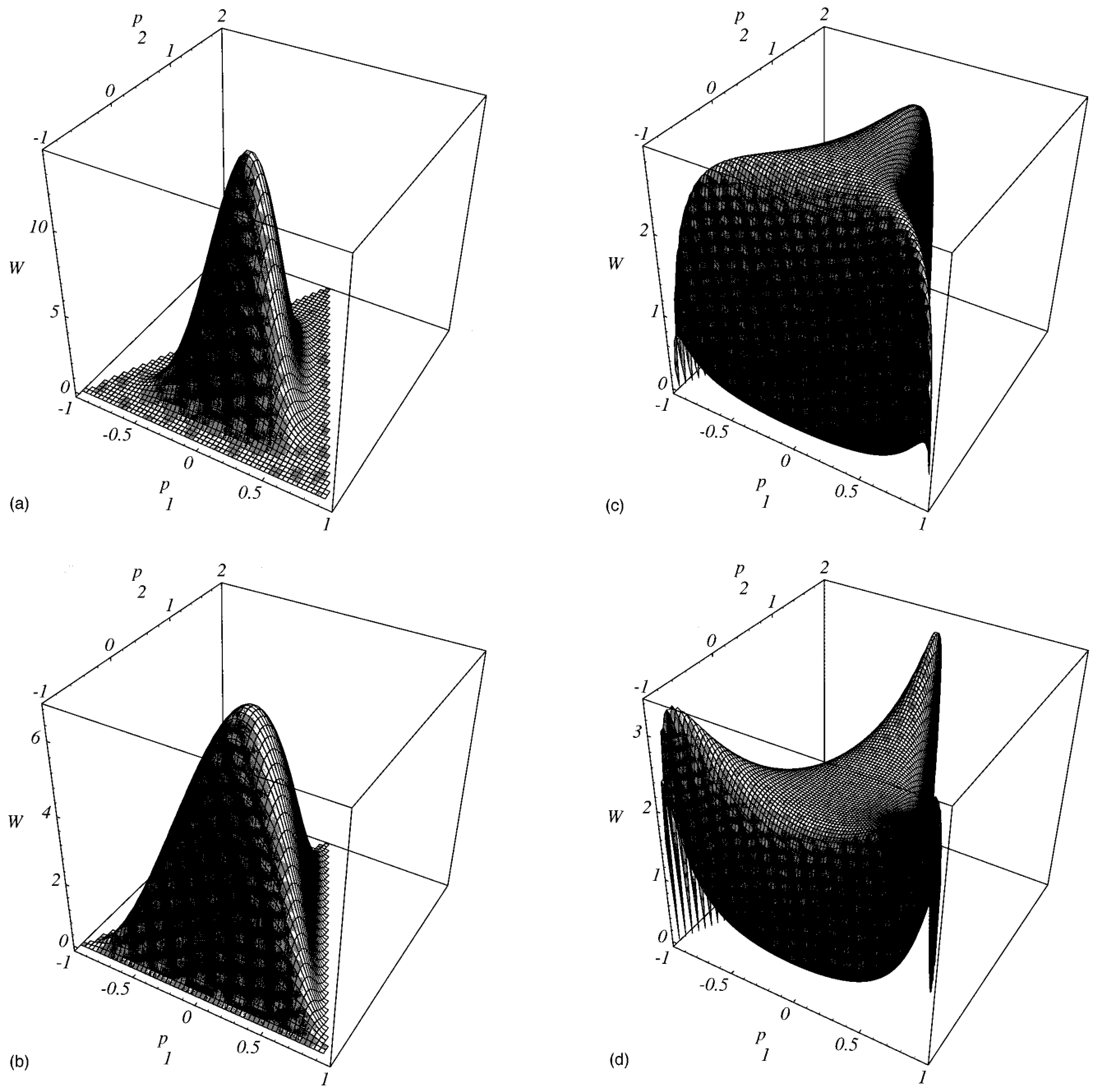

FIG. 1. The probability distribution $W(p_1,p_2)$ vs p_1,p_2 for four different values of the reduced temperature $T/J=1.5$ (a), 1.25 (b), 1.0 (c), and 0.95 (d), and for fixed $\Delta=0.1$.

introducing $\mathcal{J}\equiv\partial(x_1,x_2)/\partial(p_1,p_2)$ for the Jacobian of the transformation:

$$\mathcal{J}=\frac{36a^2/\sqrt{3}}{(p_2+1)[(p_2-2)^2-9p_1^2]}. \tag{26}$$

Combining the expressions (19)–(26) we can calculate the probability distribution $W(p_1,p_2)$ numerically. The results are shown in Fig. 1 for $\Delta=0.1$ and four different values of the reduced temperature T/J.

It should be noted that according to Eqs. (19) and (20) the components p_1 and p_2 belong to the intervals $-1\leqslant p_1\leqslant+1$ and $-1\leqslant p_2\leqslant+2$, respectively. At low temperatures the distribution $W(p_1,p_2)$ shows a three-peak structure, with the location of the peaks at (p_1,p_2) close to $(-1,-1)$, $(+1,-1)$, and $(0,+2)$. At $T=0$ the peaks would be exactly at these positions, the intensity of the last peak being exactly twice the intensity of the other two. With increasing temperature the three peaks move toward the center, and for T well above the nominal transition temperature $T_g=J$ merge into a single peak (cf. Fig. 1).

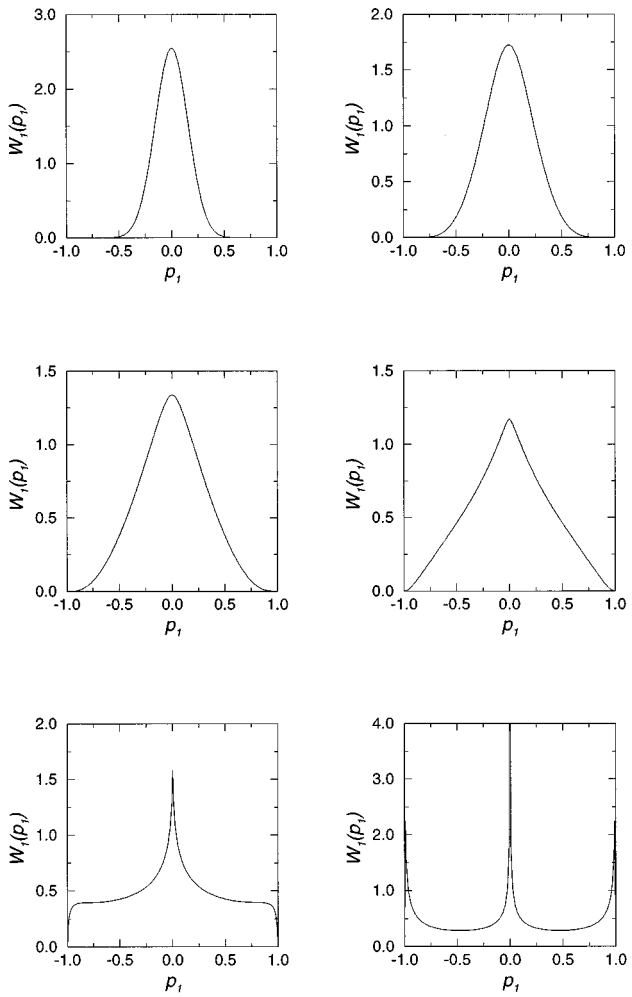

FIG. 2. Reduced probability distribution $W(p_1)$ vs p_1 defined in Eq. (27) for $\Delta=0.1$ and six values of the reduced temperature $T/J=2.0$, 1.5 (top row), 1.25, 1.0 (middle), and 0.75, 0.5 (bottom).

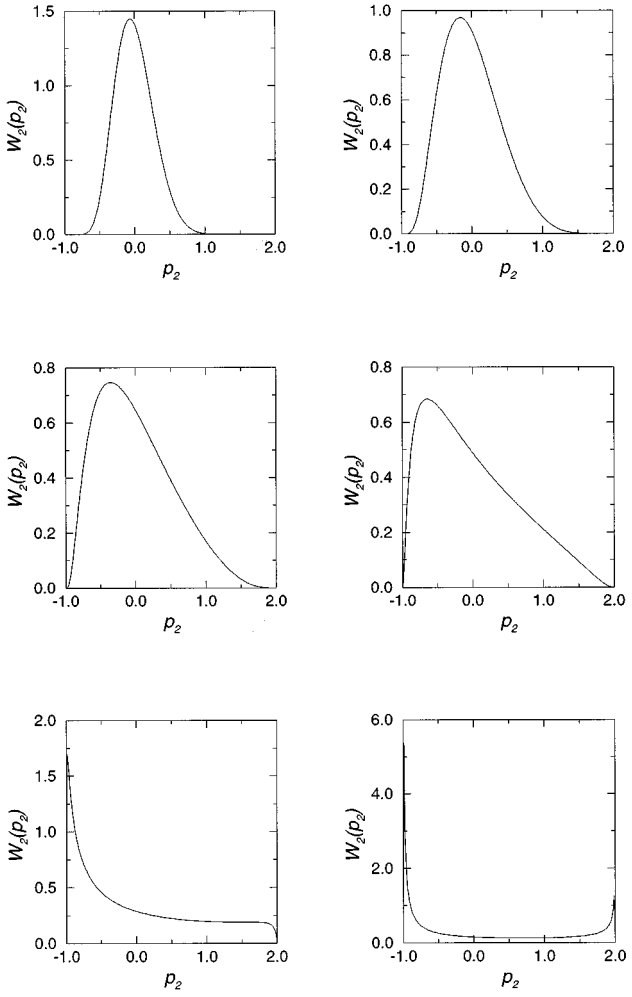

FIG. 3. Same as Fig. 2, but for the distribution $W_2(p_2)$ defined in Eq. (28).

Finally, it will be useful to define the reduced probability distributions $W_1(p_1)$ and $W_2(p_2)$,

$$W_1(p_1)=\int_{-1}^{+2} dp_2 W(p_1,p_2) \tag{27}$$

and

$$W_2(p_2)=\int_{-1}^{+1} dp_1 W(p_1,p_2), \tag{28}$$

in terms of which the EA order parameter (10) can be expressed as

$$q_\mu^{\mathrm{EA}}=\frac{1}{c_\mu^2}\int dp_\mu p_\mu^2 W_\mu(p_\mu) \quad (\mu=1,2). \tag{29}$$

The last result follows from the second of relations (15).

In Figs. 2 and 3, $W_1(p_1)$ and $W_2(p_2)$ are shown for $\Delta=0.1$ for a set of representative values of the reduced temperature T/J.

IV. RELATION TO NMR LINE SHAPE

Here we apply the theory of quadrupole-perturbed NMR (Ref. 20) to the QG system, which is described by the discrete model with equilibrium orientations of the CN molecules along the $\langle 100\rangle$, $\langle 111\rangle$, or $\langle 100\rangle$ cubic direction. We consider the case of a ^{14}N nucleus with spin $I=1$, which is rigidly connected with the CN molecule. The electric field gradient (EFG) tensor at the ^{14}N site is cylindrically symmetric and its largest principal axis V_{zz} is parallel to the C-N bond. The quadrupole-perturbed Larmor frequency of the ith ^{14}N nucleus in a cylindrically symmetric EFG tensor depends on the orientation of V_{zz} with respect to the external magnetic field $\vec{B}$ and is thus determined by the occupation probabilities N_{im}; i.e., we can write

$$\nu_i^{\pm}=\nu_L\pm\nu_K\sum_{m=1}^{s}\alpha_m\hat{N}_{im}. \tag{30}$$

Here ν_L is the unperturbed Larmor frequency and $\nu_K=3K/8$, with $K=e^2qQ/h$ standing for the ^{14}N quadrupole coupling constant.[20] Furthermore, $\alpha_m=3\cos^2\theta_m-1$, where θ_m represents the angle between the direction of the

magnetic field $\vec{B}$ and the mth equilibrium orientation of the quadrupolar axis of the CN molecule.

Using the relations (4)–(6) between $\hat{N}_{im}$ and $Z_{i\mu}$, and considering the order parameter fields as dynamic variables with instantaneous values $Z_{i\mu}(t)$, we can rewrite Eq. (30) as

$$\nu_i^{\pm}(t)=\nu_L\pm\nu_K\sum_{\mu=1}^{r} g_\mu Z_{i\mu}(t), \tag{31}$$

where we have introduced

$$g_\mu=\frac{1}{s}\sum_{m=1}^{s}\alpha_m a_{m\mu}^{T}. \tag{32}$$

The inhomogeneous NMR line shape is characterized by the average frequency distribution function[20,21]

$$I(\nu)=\frac{4}{N}\sum_i \ \mathrm{Re}\int_0^\infty dt\ e^{-i2\pi(\nu-\nu_L)t} \times\left[\left\langle \cos\left(2\pi\nu_K\sum_{\mu=1}^{r} g_\mu\int_0^t Z_{i\mu}(t')dt'\right)\right\rangle\right]_{\mathrm{av}}. \tag{33}$$

In principle, the time dependence of the variables $Z_{i\mu}(t)$ could be obtained from a dynamic model in analogy to Ising dipolar glasses;[22] however, this task is beyond the scope of the present paper. We will consider the line shape $I(\nu)$ in two limiting cases, namely, in the *slow-* and *fast-motion limits*, to be referred to as SML and FML, respectively.

A. Slow-motion limit (SML)

In the SML the jump rate $1/\tau_0$ of the CN molecules between their equilibrium orientations is much smaller than the characteristic quadrupolar frequency, i.e., $1/\tau_0\ll\nu_K$. This follows by analogy with the Glauber model of an Ising dipolar glass[22] and implies that the symmetry-adapted variables $Z_{i\mu}(t')$ in Eq. (33) can be replaced by their time-independent values $Z_{i\mu}$. Transforming back to $\hat{N}_{im}=N_{im}-1/s$ via Eq. (2) and using the fact that $N_mN_{m'}=N_m\delta_{mm'}$ and $\lim_{N\to\infty}(1/N)\Sigma_i N_{im}=1/s$, we obtain after straightforward integration,

$$I(\nu)=\frac{1}{s}\sum_{m=1}^{s}[\delta(\nu-\nu_L-\nu_K\alpha_m)+\delta(\nu-\nu_L+\nu_K\alpha_m)]. \tag{34}$$

Thus in the SML the line shape is in general given by a sum of $2s$ δ-like terms, whose frequencies depend on the orientations of the C-N bond direction with respect to the magnetic field $\vec{B}$.

The second moment of the NMR line is generally defined as

$$M_2\equiv\int_{-\infty}^{+\infty}d\nu(\nu-\nu_L)^2I(\nu). \tag{35}$$

In the SML one thus obtains from Eq. (34)

$$M_2=\frac{2}{s}\nu_K^2\sum_{m=1}^{s}\alpha_m^2. \tag{36}$$

In the following we will limit ourselves to the case of the $\langle 100\rangle$ QG model and consider three special cases of magnetic field orientation, namely, $\vec{B}$ along the [001], [110], and [$\sqrt{2}$01] directions.[23] For $\vec{B}$ along the [001] direction one has $\alpha_1=\alpha_2=-1$ and $\alpha_3=2$. Similarly, for $\vec{B}\|$[110] one finds $\alpha_1=\alpha_2=1/2$ and $\alpha_3=-1$, whereas for $\vec{B}\|$[$\sqrt{2}$01] one has $\alpha_1=1$, $\alpha_2=-1$, and $\alpha_3=0$. The corresponding values of the second moment in the SML are thus

$$M_2^{[001]}=4\nu_K^2,\quad M_2^{[110]}=\nu_K^2,\quad M_2^{[\sqrt{2}01]}=4\nu_K^2/3. \tag{37}$$

It should be noted that in the SML the ^{14}N nucleus ''sees'' the instantaneous C-N bond orientation and that one-dimensional (1D) NMR cannot be used to determine the QG order parameter q_{EA} or the quadrupolar polarization distribution. This is, however, not the case for two-dimensional (2D) exchange NMR,[24] which extends the NMR frequency observation window from 10^3–10^8 Hz into the mHz region, i.e., well into the SML. A detailed study of this technique in the case of QG's is reserved for a subsequent paper.

B. Fast-motion limit (FML)

In the FML, the average time between successive CN reorientations τ_0 is much shorter than the characteristic NMR observation time, i.e., $\tau_0\ll 1/\nu_K$. Thus the dynamic variables $Z_{i\mu}(t')$ in Eq. (33) can be replaced by their time-averaged values, which are equivalent to the local thermodynamic averages $\langle Z_{i\mu}\rangle$. Again we consider separately three relevant cases of magnetic field orientation, namely, [001], [110], and [$\sqrt{2}$01].

1. $\vec{B}\|$[001]

Here $\theta_3=0$ and $\theta_1=\theta_2=\pi/2$. Thus from Eq. (31) we have

$$\nu_i^{\pm}=\nu_L\pm\nu_Kc_2\langle Z_{i2}\rangle, \tag{38}$$

where we have used the definition (4) of the order-parameter field Z_2. Since the local thermodynamic average $\langle Z_{i2}\rangle$ plays the role of the local polarization $\hat{p}_2(\vec{x})$ introduced in Eq. (14), and $\hat{p}_2=p_2/c_2$ according to Eq. (17), the random average in Eq. (33) can be evaluated as an integral over the corresponding probability distribution $W_2(p_2)$. Equation (38) suggests that the symmetry-adapted order-parameter field Z_{i2} is a physical observable in the FML.

Combining Eqs. (16), (28), (33), and (38) we obtain the relation

$$I(\nu)=\frac{1}{\nu_K}\left[W_2\left(\frac{\nu-\nu_L}{\nu_K}\right)+W_2\left(\frac{\nu_L-\nu}{\nu_K}\right)\right]. \tag{39}$$

This can also be expressed in differential form

$$I(\nu)d\nu=W_s(p_2)dp_2, \tag{40}$$

where we have introduced the symmetrized probability distribution $W_s(p_2)\equiv[W_2(p_2)+W_2(-p_2)]$. From the mea-

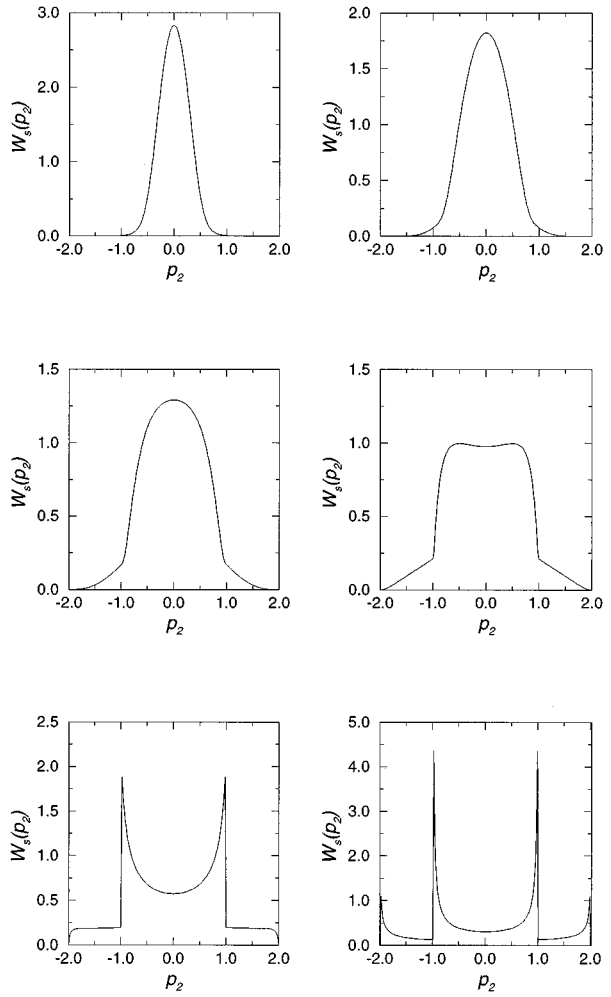

FIG. 4. Symmetrized probability distribution $W_s(p_2) = W_2(p_2) + W_2(-p_2)$ for the same set of parameters as in Figs. 2 and 3.

sured NMR line shape one can thus simply deduce the probability distribution of local quadrupolar polarization $W_s(p_2)$ and compare it with model calculations. In Fig. 4 the calculated distribution $W_s(p_2)$ is plotted for six different temperatures.

From Eq. (39) one can easily evaluate the observable second moment of the NMR line. The result is

$$M_2^{[001]} = 2\,\nu_K^2 \int dp_2 p_2^2 W_2(p_2) = 4\,\nu_K^2 q_{\mathrm{EA}}, \tag{41}$$

where the last relation follows from Eq. (29). This shows that the order parameter q_{EA} and its temperature dependence can be simply obtained from the second moment of the measured NMR line shape. It should be noted that the exact value of M_2, i.e., the one obtained by integrating over an infinite frequency interval, is not affected by molecular motion and should always be given by the general result (36).[20] This is, however, not observable. Expression (41) differs from Eq. (36) by the factor q_{EA}, because the high-frequency part of the spectrum has been eliminated in replacing the time dependence of the local polarization by its long-time average value. Experimentally, the same reduction of M_2 is accomplished by cutting off the integration at some large enough frequency $\nu_{\max}$,[22] such that no obervable part of the NMR spectrum exists for $\nu > \nu_{\max}$.

2. *Case* $\vec{B}$||[110]

Now $\theta_3 = \pi/2$ and $\theta_1 = \theta_2 = \pi/4$. From Eq. (30) one finds

$$\nu_i^{\pm} = \nu_L \mp \tfrac{1}{2}\nu_K c_2 \langle Z_{i2} \rangle, \tag{42}$$

and the relation between $I(\nu)$ and $W_2(p_2)$ is thus analogous to the previous case as given by Eq. (39), but with ν_K replaced by $\nu_K/2$. In particular, the second moment of the NMR line shape is now given by

$$M_2^{[110]} = \nu_K^2 q_{\mathrm{EA}}. \tag{43}$$

3. *Case* $\vec{B}$||[$\sqrt{2}$01]

In this case $\theta_2 = \pi/2$; i.e., $\vec{B}$ lies in the (x,z) plane at $\theta_1 = 54.7°$ (i.e., magic angle) and $\theta_3 = 35.3°$. Thus Eq. (30) yields

$$\nu_i^{\pm} = \nu_L \pm \nu_K c_1 \langle Z_{i1} \rangle, \tag{44}$$

leading to the following results for the line shape,

$$I(\nu) = \frac{2}{\nu_K} W_1\left(\frac{\nu - \nu_L}{\nu_K} \right), \tag{45}$$

and its second moment:

$$M_2^{[\sqrt{2}01]} = \tfrac{4}{3}\nu_K^2 q_{\mathrm{EA}}. \tag{46}$$

By performing an experiment with the above orientation of the magnetic field one thus has the possibility to determine the probability distribution $W_1(p_1)$.

V. DISCUSSION AND CONCLUSIONS

We have presented a calculation of the local quadrupolar polarization distribution $W(p_1,p_2)$ in quadrupolar glasses (QG's) with pseudocubic symmetry and equilibrium orientations of the quadrupolar axis along the $\langle 100 \rangle$ directions. The investigation is based on the semimicroscopic symmetry adapted random-bond random-field (SARBRF) model of QG's within the framework of a replica mean-field theory. The model contains two physical parameters, i.e., the random-bond and random-field strengths J and Δ, respectively. In the $\langle 100 \rangle$ or $r=2$ case there are two nontrivial components of the local polarization, namely, p_1 and p_2 corresponding to the symmetry-adapted order-parameter fields $Z_{i\mu}$ ($\mu = 1,2$), and one has in the replica-symmetric phase a single QG order parameter q.

The results are applicable to QG's with strong crystal anisotropy such as $(\mathrm{NaCN})_{1-x}(\mathrm{KCN})_x$, $\mathrm{KBr}_{1-x}(\mathrm{CN})_x$, and related systems. A powerful experimental method to investigate the QG ordering in these systems is the quadrupole-perturbed NMR of the ^{14}N nucleus of the CN molecule. In the fast motion limit (FML) and for magnetic field $\vec{B}$ along the [100] or [110] direction, the NMR spectrum is given by the symmetrized form of the reduced local polarization distribution $W_2(p_2) = \int W(p_1,p_2)dp_1$. For $\vec{B}$||[$\sqrt{2}$01], how-

ever, the line shape is determined by $W_1(p_1)=\int W(p_1,p_2)dp_2$. Preliminary results for $\vec{B}||[100]$ and $\vec{B}||[110]$ show a qualitative agreement[18] with the predicted line shape in the FML as shown in Fig. 4 for $T/J=0.75$. The case $\vec{B}||[\sqrt{2}01]$ has not yet been investigated experimentally. For temperatures much higher than the potential anisotropy, other orientations of the CN molecules besides $\langle 100\rangle$ will become populated. Therefore, the $r=2$ model cannot be expected to provide a detailed description of the system, and should be generalized to a combination of the $r=2$, 3, and 5 discrete models, or even replaced by the much more complicated continuous hindered-rotation model.[7]

In the FML, the observable second moment of the NMR line M_2 is proportional to the quadrupolar Edwards-Anderson order parameter q_{EA}. Thus by measuring M_2 at various temperatures one can determine the temperature dependence of q_{EA}. In this paper we present the results of a replica theory based on the SARBRF model, from which one can readily calculate the replica-symmetric QG order parameter q for the three relevant cases of quadrupolar orientation. As already noted in Ref. 15, an approximate theory based on the Ising RBRF model of dipolar glasses provides a very good estimate of the temperature dependence of the order parameter q.[17] By relating q_{EA} to the theoretical value of $q(T)$ within the SARBRF model in the replica-symmetric phase, one should be able to determine more precisely the values of the model parameters J and Δ, from which the freezing temperature T_f can then be calculated.[15]

Below T_f, replica symmetry is broken and q_{EA} should be related to the corresponding Parisi order parameter function $q(x)$.[14] The analogy with dipolar glasses suggests, however, that the effects of broken replica symmetry on $q(x)$ are rather small, and it is thus unlikely that they could be observed experimentally.

An interesting problem is the crossover between the FML and SML on lowering the temperature. It seems plausible to assume that the CN reorientation time obeys an Arrhenius law of the type $\tau_0=\tau_\infty\exp(E_a/kT)$,[22] where the parameters τ_∞ and E_a could be estimated from the ^{14}N-T_1 data. Since $\nu_K\approx 1.5\times 10^6$ Hz,[18] the FML condition $\tau_0\nu_K\ll 1$ is easily satisfied at temperatures much above the the freezing temperature T_f, which is about ~ 110 K in $(\mathrm{NaCN})_{0.41}(\mathrm{KCN})_{0.59}$ and ~ 64 K in $(\mathrm{KBr})_{0.47}(\mathrm{KCN})_{0.53}$.[9] As the temperature is lowered, τ_0 increases and the SML is reached at some point, resulting in a gradual increase of M_2 towards its maximum value. One expects no dramatic changes in M_2 to occur at T_f, since the individual CN reorientations are going on even in the frozen phase and thus τ_0 does not diverge at the transition. This is to be contrasted with the behavior of the dynamic response function $G(\omega)$,[19] which can be characterized by an effective relaxation time $\tau_{\mathrm{eff}}\propto -i\lim_{\omega\to 0}\partial G(\omega)/\partial\omega$. On approaching T_f from above τ_{eff} diverges, giving rise to some typical glassy phenomena like the splitting between the field-cooled and zero-field-cooled elastic susceptibilities and the divergence of the nonlinear susceptibilities.[9]

It would be interesting to test the predictions of the present work by analyzing the NMR spectra of the mixed cyanides and then use the values of the model parameters to calculate other physical properties of these systems.

ACKNOWLEDGMENT

This work was supported by the Ministry of Science and Technology of the Republic of Slovenia.

[1] U.T. Höchli, K. Knorr, and A. Loidl, Adv. Phys. **39**, 405 (1990).
[2] K. Binder and J.D. Reger, Adv. Phys. **41**, 547 (1992).
[3] K.H. Michel and J.M. Rowe, Phys. Rev. B **22**, 1417 (1980).
[4] N.S. Sullivan, M. Devoret, B.P. Cowan, and C. Urbina, Phys. Rev. B **17**, 5061 (1978).
[5] A. Brooks Harris and H. Meyer, Can. J. Phys. **63**, 3 (1985).
[6] H. Vollmayr, R. Kree, and A. Zippelius, Phys. Rev. B **44**, 12 238 (1991).
[7] K. Walasek and K. Lukierska-Walasek, Phys. Rev. B **48**, 12 550 (1993).
[8] B. Tadić, R. Pirc, R. Blinc, J. Petersson, and W. Wiotte, Phys. Rev. B **50**, 9824 (1994).
[9] J. Hessinger and K. Knorr, Phys. Rev. Lett. **63**, 2749 (1990); *ibid.* **65**, 2674 (1992); Phys. Rev. B **47**, 14 813 (1993).
[10] T. Schräder, A. Loidl, G.J. McIntyre, and C.M.E. Zeyen, Phys. Rev. B **42**, 3711 (1990).
[11] K.H. Michel, Phys. Rev. Lett. **57**, 2188 (1986); Phys. Rev. B **35**, 1405 (1987).
[12] L.J. Lewis and M.L. Klein, Phys. Rev. Lett. **57**, 2698 (1986).
[13] R. Pirc, B.Tadić, and R. Blinc, Phys. Rev. B **36**, 8607 (1987).
[14] K.H. Fischer and J.A. Hertz, *Spin Glasses* (Cambridge University Press, Cambridge, England, 1991).
[15] R. Pirc, B.Tadić, and R. Blinc, Ferroelectrics **183**, 235 (1996).
[16] R. Blinc, J. Dolinšek, R. Pirc, B. Tadić, B. Zalar, R. Kind, and O. Liechti, Phys. Rev. Lett. **63**, 2248 (1989).
[17] W. Wiotte, J. Petersson, R. Blinc, and S. Elschner, Phys. Rev. B **43**, 12 751 (1991).
[18] B. Zalar and J. Petersson (unpublished).
[19] R. Pirc and B. Tadić, Phys. Rev. B **54**, 7121 (1996).
[20] A. Abragam, *The Principles of Nuclear Magnetism* (Clarendon Press, Oxford, 1986).
[21] S. Dattagupta, *Relaxation Phenomena in Condensed Matter Physics* (Academic, London, 1987).
[22] R. Pirc, B. Tadić, R. Blinc, and R. Kind, Phys. Rev. B **43**, 1501 (1991).
[23] Note that for $\vec{B}||[111]$ there is no frequency shift in the $\langle 100\rangle$ model.
[24] J. Dolinšek, B. Zalar, and R. Blinc, Phys. Rev. B **50**, 805 (1994).